

# Interaction Properties of the Periodic and Step-like Solutions of the Double-Sine-Gordon Equation

M. Peyravi<sup>1</sup>, Afshin Montakhab<sup>2\*</sup>, N. Riazi<sup>1†</sup> and A. Gharaati<sup>3</sup>

1. *Physics Department and Biruni Observatory , Shiraz University, Shiraz 71454, Iran,*
2. *Physics Department, Shiraz University, Shiraz 71454, Iran,*
3. *Physics Department, Payame Noor University, Shiraz, Iran.*

The periodic and step-like solutions of the double-Sine-Gordon equation are investigated, with different initial conditions and for various values of the potential parameter  $\epsilon$ . We plot energy and force diagrams, as functions of the inter-soliton distance for such solutions. This allows us to consider our system as an interacting many-body system in  $1 + 1$  dimension. We therefore plot state diagrams (pressure vs. average density) for step-like as well as periodic solutions. Step-like solutions are shown to behave similarly to their counterparts in the Sine-Gordon system. However, periodic solutions show a fundamentally different behavior as the parameter  $\epsilon$  is increased. We show that two distinct phases of periodic solutions exist which exhibit manifestly different behavior. Response functions for these phases are shown to behave differently, joining at an apparent phase transition point.

PACS: 05.45.Yv, 05.00.00, 02.60.Lj, 24.10.Jv

## I. INTRODUCTION

The Sine-Gordon (SG) equation is a non-linear partial differential equation which appears naturally in different physical systems in atomic physics [1], electromagnetism[2], superconductivity[3], field theory[4], biophysics[5, 6, 7], and statistical mechanics[8].

The double-Sine-Gordon (DSG) equation which is a generalization of the ordinary SG equation has been the focus of much recent investigations. It has been shown to model a variety of systems in condensed matter, quantum optics, and particle physics[9]. Condensed-matter applications include the spin dynamics of superfluid  $^3He$ [10, 11], magnetic chains[12], commensurate-incommensurate phase transitions[13], surface structural reconstructions[14], domain walls[15, 16] and fluxon dynamics in Josephson junction[17].

In quantum field theory and quantum optics DSG applications include quark confinement[18]

---

\* email: montakhab@shirazu.ac.ir

† email: riazi@physics.susc.ac.ir

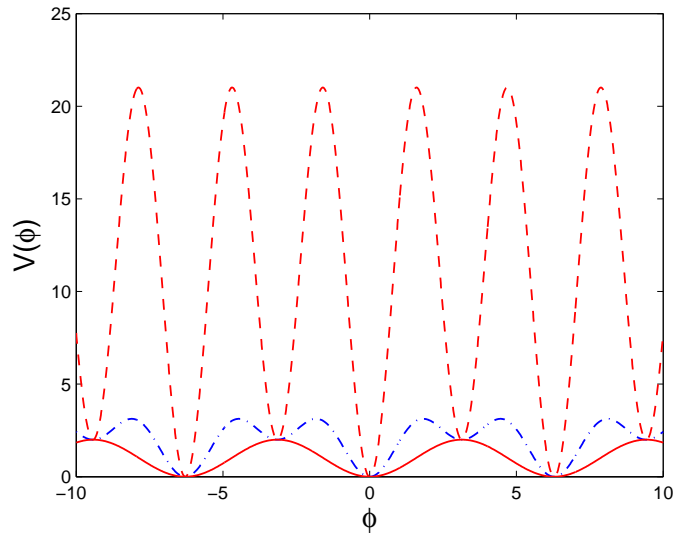


FIG. 1: DSG Potential. The dashed curve is for  $\epsilon = 10$ , the dash-dotted curve is for  $\epsilon = 1$  and the solid curve is for  $\epsilon = 0$ (SG).

and self-induced transparency[19]. The internal dynamics of multiple and single DSG soliton configurations using molecular dynamics have been studied in[9]. There have also been studies about kink anti-kink collision processes for DSG equation [20]. One can also point to the statistical mechanical applications[21], and perturbation theory for this equation[22]. It should be mentioned that the potentials adopted in various studies are not exactly the same. The DSG potential which contains a constant and a harmonic term in addition to the self-interaction potential of the ordinary SG equation is considered here[22, 23]:

$$V(\phi) = 1 + \epsilon - \cos \phi - \epsilon \cos(2\phi). \quad (1)$$

where  $\epsilon$  is a constant. This potential is sketched in Fig.1 for  $\epsilon = 0, 1$  and 10. Some dynamical properties of multiple and single soliton solutions of the DSG system were studied by Burdick et. al[9], using molecular dynamics.

Following the common terminology in field theory, this potential has absolute degenerate minima at  $\phi = 2n\pi$  as the true vacua, and the metastable, local minima at  $\phi = (2n + 1)\pi$  as the false vacua[23]. False vacua develop if  $\epsilon > 0.25$ [23]. The harmonic term in this potential can result from the Fourier expansion of an arbitrary, periodic potential  $\tilde{V}(\phi) = \tilde{V}(\phi + 2n\pi)$ . One does not expect the system to remain integrable by adding these extra terms[23]. The potential reduces to the ordinary SG potential in the limit  $\epsilon \rightarrow 0$ .

In this article, we consider chains of the kink and anti-kink solutions of DSG equation in 1 + 1

dimension. Our goal is to consider a one dimensional chain of many solitons and treat them as a many-body interacting system. As will be shown shortly, these solutions do have mutual interactions which is a function of their mutual distance. We thus propose to study the DSG system as a many-body interacting system at zero temperature in one spatial dimension.

The structure of our presentation is as follows: in Section II we review some basic properties of the DSG system. In Section III, we study the periodic and step-like solutions of the DSG system, highlighting their interaction properties. In Section IV, we study the macroscopic properties of such systems viewed as a many-body interacting system. We close in Section V by summarizing our results and pointing some directions for future work.

## II. BASIC PROPERTIES OF THE DOUBLE SINE-GORDON SYSTEM

From a relativistic point of view, the double-Sine-Gordon Lagrangian density can be put in the following form:

$$\mathcal{L}_{DSG} = \frac{1}{2} \partial^\mu \phi \partial_\mu \phi - [1 + \epsilon - \cos \phi - \epsilon \cos(2\phi)]. \quad (2)$$

From this Lagrangian density, we obtain the following equation:

$$\square \phi = -\sin \phi - 2\epsilon \sin(2\phi); \quad (3)$$

for the real scalar field  $\phi(x, t)$  in  $(1 + 1)$  dimensions. It can be shown that this equation has the following exact, static, single kink (anti-kink) solution[23]:

$$\phi(x) = 2 \arccos \left[ \pm \frac{\sinh \sqrt{4\epsilon + 1} x}{\sqrt{4\epsilon + \cosh^2 \sqrt{4\epsilon + 1} x}} \right]. \quad (4)$$

These are plotted in Fig.2 for three values of the parameter  $\epsilon (= 0, 1, 10)$ . Note that the (+) sign is for the anti-kink ( $\tilde{k}$ ), while the (-) sign is for the kink ( $k$ ). The solution (4) tends to the conventional kink (anti-kink) solution of the SG equation in the limit  $\epsilon \rightarrow 0$ . As the value of  $\epsilon$  grows, the kink develops two parts (or sub-kinks)[23], see Fig.3.

Exact solutions of DSG system with arbitrary constant coefficients were obtained recently by Wang and Lie[24] by F-expansion method which is a generalization of the Jacobi elliptic function expansion. It is obvious that solitary and periodic solutions of the SG system are special cases of these solutions (with particular choices of the constants of integration). The thermodynamic properties of the DSG chain were studied in Condat et. al[25], in which the polarization precursor was determined.

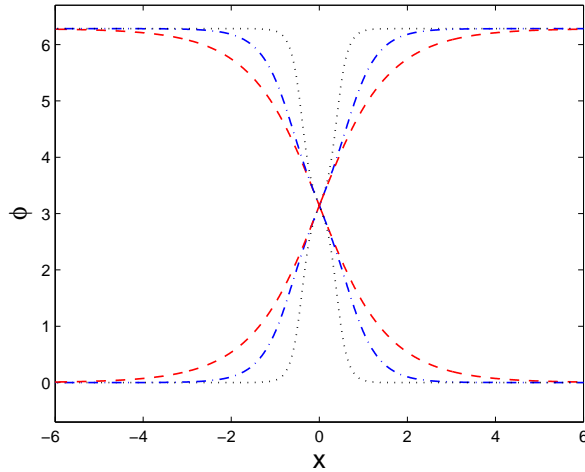


FIG. 2: Kink and anti-kink solutions of DSG. The dotted curves are for  $\epsilon = 10$ , the dash-dotted curves are for  $\epsilon = 1$  and the dashed curves are for  $\epsilon = 0$ (SG).

Using the Noether's theorem and the invariance of the action under the the space-time translation  $x^\mu \rightarrow^\mu + a^\mu$ , one easily obtains[26, 27]:

$$T^{\mu\nu} = \partial^\mu \phi \partial^\nu \phi - g^{\mu\nu} \mathcal{L}_{DSG}; \quad (5)$$

in which  $g^{\mu\nu} = \text{diag}(1, -1)$  is the metric of the  $(1 + 1)$  dimensional Minkowski spacetime. The energy-momentum tensor of the true vacuum ( $\phi = 2n\pi$ ) vanishes, while for the false vacuum ( $\phi = (2n + 1)\pi$ ), it is non-vanishing[23]:

$$T^{\mu\nu} = 2g^{\mu\nu}. \quad (6)$$

As expected, this tensor is that of a perfect fluid, with the equation of state  $p = -\rho = -2$ [23], similar to that of the cosmological constant[27]. Using the virial theorem, the energy density of the static kink is given by (see Fig.3):

$$\mathcal{H}(x) = 2V(\phi) = 2[1 + \epsilon - \cos(\phi(x)) - \epsilon \cos(2\phi(x))]. \quad (7)$$

As for the SG system, the topological current for the DSG system is given by[28]:

$$J^\mu = \frac{1}{2\pi} \epsilon^{\mu\nu} \partial_\nu \phi; \quad (8)$$

where  $\epsilon^{\mu\nu}$  is the totally antisymmetric tensor in two dimensions. The current density (8) is conserved:

$$\partial_\mu J^\mu = \frac{1}{2\pi} \epsilon^{\mu\nu} \partial_\mu \partial_\nu \phi = 0. \quad (9)$$

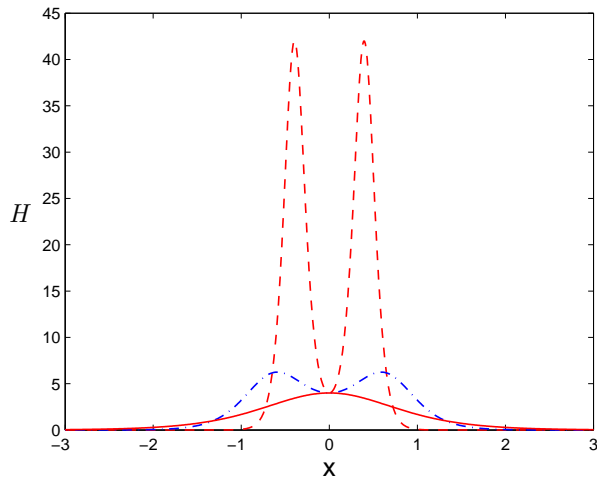


FIG. 3: DSG energy density for the kink solution. The dashed curve is for  $\epsilon = 10$ , the dash-dotted curve is for  $\epsilon = 1$  and the solid curve is for  $\epsilon = 0$ (SG). It can be seen that sub-kinks develop for large enough values of  $\epsilon$  ( $\epsilon > 0.25$ )

since  $\epsilon^{\mu\nu}$  is antisymmetric while  $\partial_\mu\partial_\nu$  is symmetric in the indices. The total topological charge of a localized solution is given by:

$$\begin{aligned} Q &= \int_{-\infty}^{+\infty} J^0 dx = \frac{1}{2\pi} \int_{-\infty}^{+\infty} \epsilon^{01} \partial_1 \phi dx \\ &= \frac{1}{2\pi} \int_{-\infty}^{+\infty} \frac{\partial \phi}{\partial x} dx = \frac{1}{2\pi} [\phi(+\infty) - \phi(-\infty)]. \end{aligned} \quad (10)$$

Considering the boundary conditions of a localized solution, the DSG equation leads to:

$$\phi(+\infty) = 2n\pi, \quad \phi(-\infty) = 2m\pi; \quad Q = n - m. \quad (11)$$

Localized, static solutions have  $n - m = \pm 2\pi$ , and therefore

$$Q = \pm 1 \quad \text{for kink (anti-kink)}. \quad (12)$$

As the value of  $\epsilon$  grows, sub-kinks form, which have half-integral topological charges[23].

The stability of kink solutions of the DSG system is guaranteed by topological reasons. The kink is the lowest energy configuration with the prescribed boundary conditions and the topological charge given by Eq.(12).

### III. PERIODIC AND STEP-LIKE SOLUTIONS

In this section, we classify and study two types of static solutions of the DSG equation, for which we have:

$$\frac{d^2\phi}{dx^2} = \frac{dV(\phi)}{d\phi}. \quad (13)$$

In order to proceed, we use a Runge-Kutta method[29] to integrate Eq. (13) numerically. We choose  $\phi = \pi$  and various values of  $\frac{d\phi}{dx}$  as our initial conditions at  $x = 0$ . We study this system for various potential parameters  $\epsilon$ . We choose  $\epsilon = 1$  as a typical value but also compare results with  $\epsilon = 0.1$  (SG-like behavior) as well as  $\epsilon = 10$  for decidedly different behavior. It is easy to see that solutions are characterized by an ( $x$ -independent) constant  $P$ :

$$P = \frac{1}{2} \left( \frac{d\phi}{dx} \right)^2 - V(\phi); \quad (14)$$

$$\frac{dP}{dx} = 0. \quad (15)$$

Note that this is different from energy density

$$\mathcal{H}(x) = \frac{1}{2} \left( \frac{d\phi}{dx} \right)^2 + V(\phi); \quad (16)$$

which changes with position  $x$ . We will interpret  $P$  as “pressure” (or tension in this 1d case) for reasons to be explained in the next section.

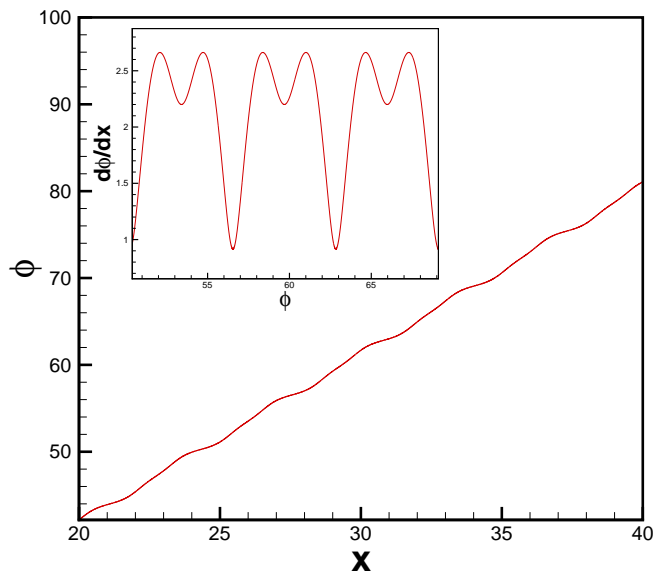


FIG. 4: Step-like chain of DSG solitons for  $\epsilon = 1$  and  $P = 0.42$ . The inset shows the cyclic nature of these solutions in more details.

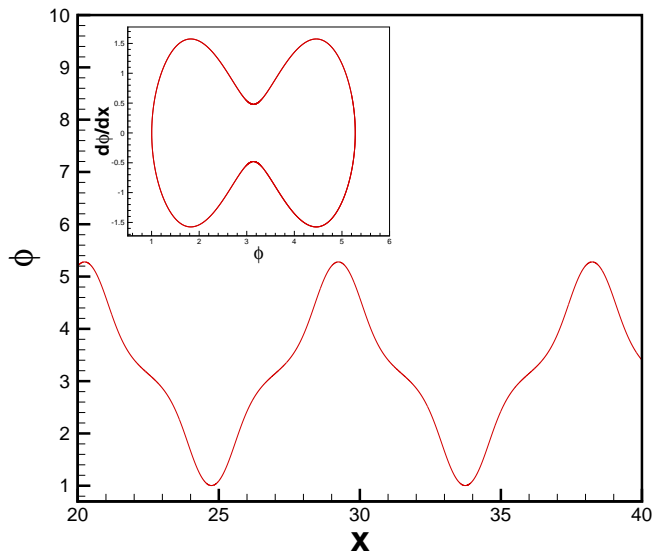


FIG. 5: Periodic chain of DSG solitons for  $\epsilon = 1$  and  $P = -1.8848$ . The inset shows the cyclic nature of these solutions in more details.

Two types of solutions emerge under such conditions: Step-like solutions and periodic solutions (see Fig.4 and 5). Step-like solutions are characterized by  $P > 0$  and periodic solutions are characterized for  $-2 < P < 0$ . Note that this classification is independent of  $\epsilon$  and therefore holds true also for SG equation[30]. As can be seen from the relevant figures the step-like solutions are a sequence of kinks ( $kkk\dots$ ) or anti-kinks ( $\tilde{k}\tilde{k}\tilde{k}\dots$ ), and the periodic solutions are a sequence of kink, anti-kink ( $k\tilde{k}k\tilde{k}\dots$ ) solutions. A simple phase diagram of Eq. (13) is shown in Fig. 6.

Using Eq.(16), one can characterize these solutions via an energy function. We take a given static solution and compute the total energy per “soliton” i.e. integral of Eq.(16) over one period. For each static solution we also calculate the “inter-soliton” distance,  $L$ , as a distance between two successive (similar) peaks of energy density. We can therefore plot energy per soliton as a function of inter-soliton distance for various values of  $\epsilon$  and  $P$ . Since it is our goal to consider these systems as a many-body system, we use energy as a function of distance  $E(L)$  and compute the “inter-soliton force”  $F = -\frac{dE}{dL}$ . Figure 7 shows such results for the step-like solutions. No significant change of behavior is seen as  $\epsilon$  is varied for these type of solutions. We note that in both cases (SG and DSG) at short distances the energy rises abruptly reminiscent of hard core potentials. It quickly falls as distance  $L$  is increased reaching an asymptotic value for large  $L$ . Accordingly, the “inter-soliton force”  $F$  (insets) is repulsive and falls to zero quickly as distance is increased,

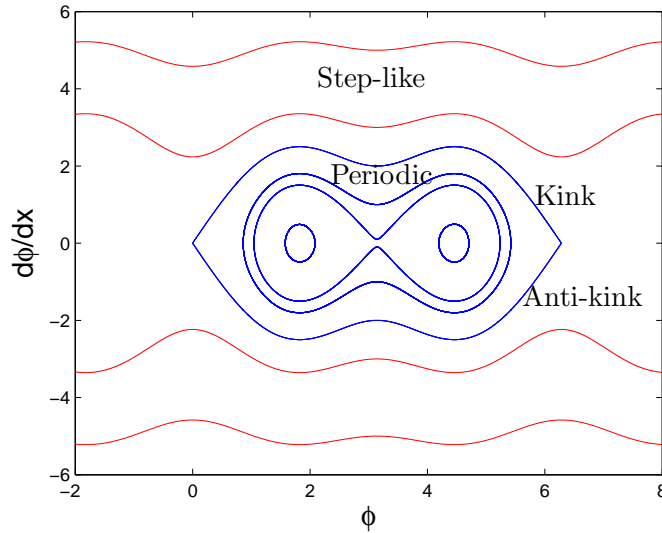


FIG. 6: A typical phase diagram for solutions of Eq. (13) with  $\epsilon = 1.0$ . The two different solutions are clearly marked on the diagram.

indicating a short-range interaction.

We next consider the periodic solutions. Here, as we will show,  $\epsilon$  changes the behavior of these solutions in a significant way. Figure 8 shows the results for the periodic solutions for  $\epsilon = 0$  (SG). The behavior is the reverse of the step-like solutions. The energy decreases sharply at short distances and increases quickly to a constant value at large  $L$ . Therefore, the inter-soliton force is attractive and falls off to zero at large distances (inset). What happens as  $\epsilon$  is changed in this case? The results for the energy diagram is shown in Fig.9. As is seen from the figure, the introduction of  $\epsilon$  leads to the emergence and growth of a new branch of solutions. It is important to distinguish between these two types of periodic solutions. The inter-soliton distance  $L$  changes with  $P$  which is a function of initial conditions. In the lower branch (the SG-like branch), as  $L$  becomes large, the energy per soliton tends to its single-soliton value, thus leading to an independent soliton system. However, in the upper branch, as  $L$  become large the sub-kinks also separate out with a false vacuum energy developing between them. Here, as  $L$  grows large, the total energy in the false vacua increases linearly in the space between the sub-kinks, which is indicated by the linear dependence of energy in Fig.9[31]. To help visualize these different solutions, we show in Fig.10 a periodic solution from each branch, having the same  $L$  but different  $E$ . The inter-soliton force for the periodic solution is still attractive since in either branch the energy is an increasing function of distance. However, in the lower (SG like) branch the force falls off to zero at large distances leading to a non-interacting soliton picture. Note that this is the case in all the solutions considered thus



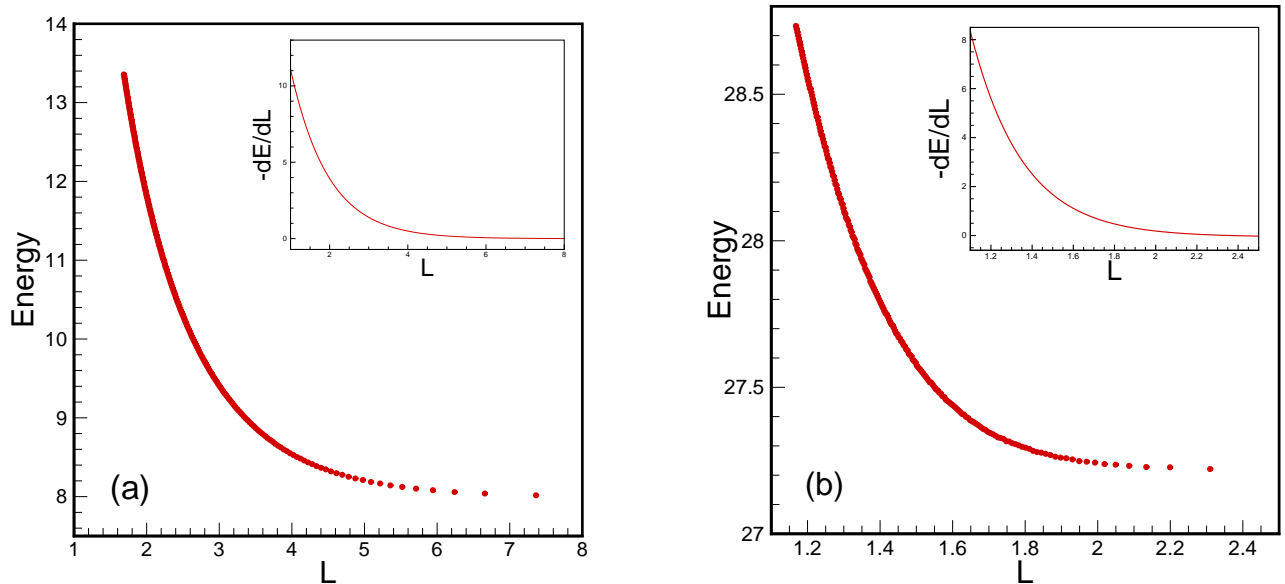


FIG. 7: Energy per soliton diagram for step-like chain of (a) SG solitons and (b) DSG solitons for  $\epsilon = 10$ . The behavior of the system does not change significantly as  $\epsilon$  is changed. The inset shows the derivative which we interpret as the (repulsive) force between the solitons.

far. But, in the new upper branch, the attractive force increases its (absolute) values to  $-2$  as  $L$  is increased (Fig.10b). This is due to the above-mentioned linear behavior of energy in the upper branch, caused by separation of sub-kinks with increasing  $L$ . A typical force diagram for periodic solution of DSG system with  $\epsilon = 1$  is shown in Fig.11

#### IV. PERIODIC AND STEP-LIKE SOLUTIONS AS A MANY-BODY SYSTEM

In order to gain a better understanding of the soliton interpretation and mutual interactions between solitons, one may also study state diagrams which depict pressure  $P$  versus average density  $\bar{\rho}$ , where  $P$  and  $\rho$  are given by[32]:

$$P = -T_1^1 = \frac{1}{2} \left( \frac{\partial \phi}{\partial x} \right)^2 - V(\phi). \quad (17)$$

$$\rho = T_0^0 = \frac{1}{2} \left( \frac{\partial \phi}{\partial x} \right)^2 + V(\phi). \quad (18)$$

It should be noted that the energy-momentum tensor of the system (like many other relativistic

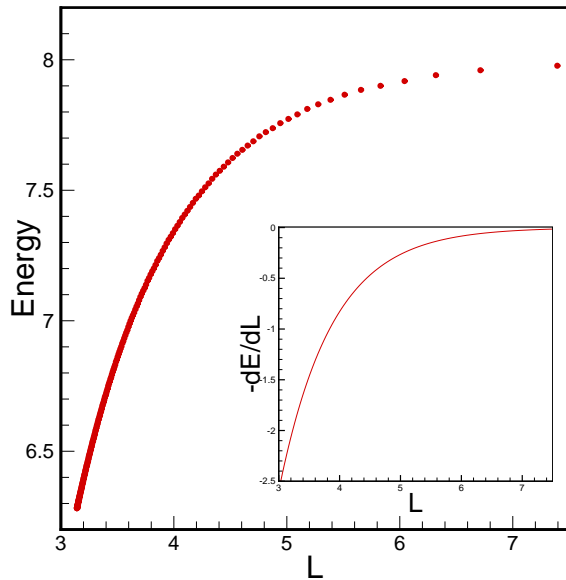


FIG. 8: Energy per soliton diagram for periodic chain of the SG solitons. The inset shows the derivative which we interpret as the (attractive) force between the solitons.

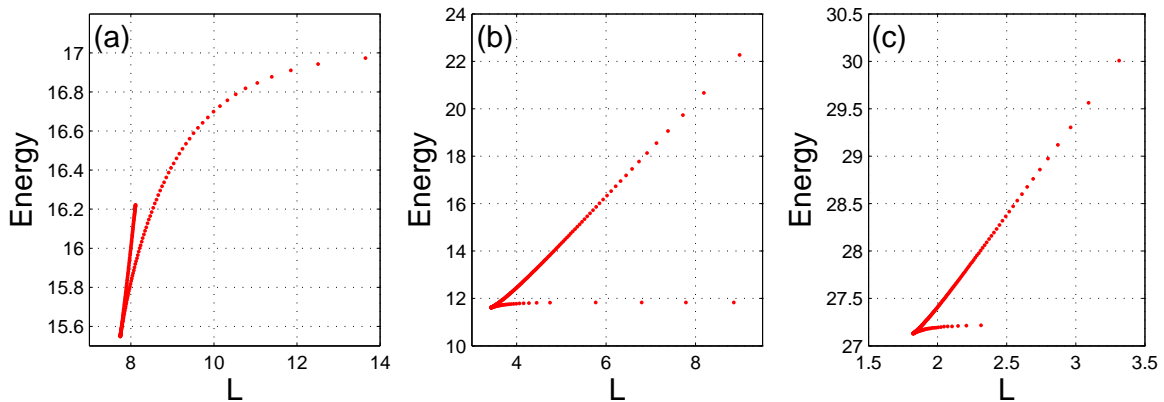


FIG. 9: Energy per soliton diagram for periodic chain of DSG solitons (a) for  $\epsilon = 0.1$ , (b) for  $\epsilon = 1$  and (c) for  $\epsilon = 10$ . Note the emergence of a new (upper) branch as  $\epsilon$  is increased. The lower branch reaches a constant value for large  $L$ , but the upper branch increases linearly with slope 2.

continuous media) takes the form

$$(T_\nu^\mu) = \begin{pmatrix} T_0^0 & 0 \\ 0 & T_1^1 \end{pmatrix} \quad (19)$$

reminiscent of the energy-momentum tensor of a perfect fluid in  $1 + 1$  dimensions given by[32]:

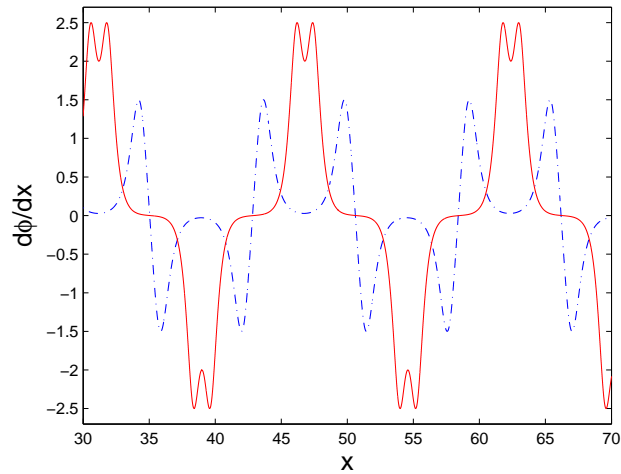


FIG. 10: The slope diagram for the periodic chain of DSG solitons for  $\epsilon = 1$ , with  $P = -2.14 \times 10^{-5}$  for the curve with larger amplitude (solid curve) and with  $P = -1.9996$  for the curve with smaller amplitude (dash-dotted curve). The two solutions have the same inter-soliton distance ( $L=7.798$ ) but different energy per soliton.

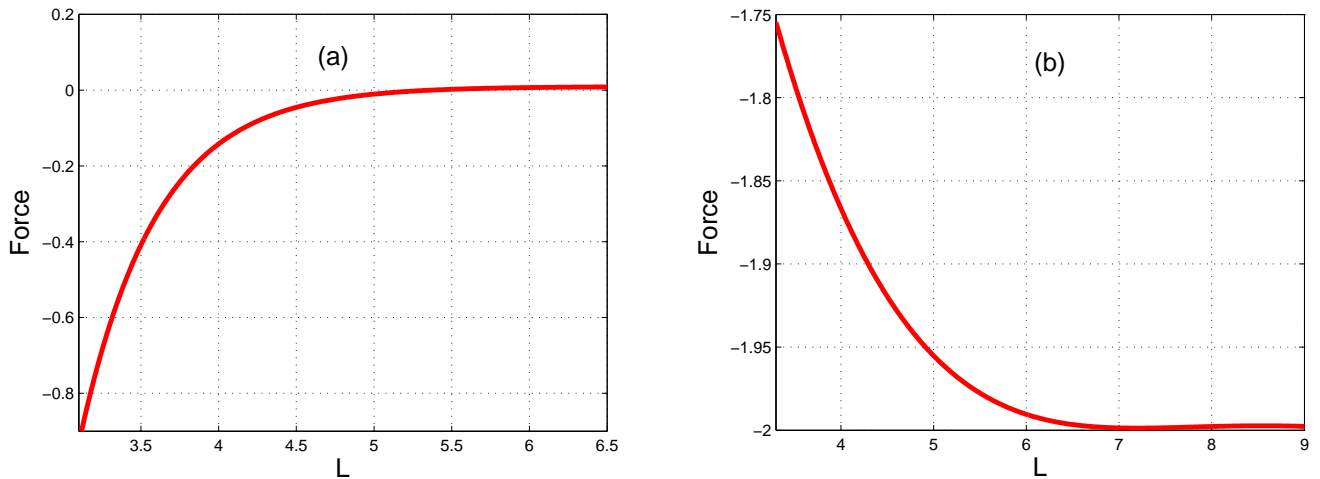


FIG. 11: Attractive force for: (a) the lower branch and (b) the upper branch of periodic chain of DSG solitons for  $\epsilon = 1$ .

$$(T_{\nu}^{\mu}) = \begin{pmatrix} \rho c^2 & 0 \\ 0 & -P \end{pmatrix} \quad (20)$$

Note that pressure is the same as our first integral  $P$  (Eq.(14)) and density  $\rho$  is in fact the same as energy (Hamiltonian) density (Eq.(16)). Here we use the generic word “pressure” as a thermodynamic conjugate variable to the size of the system. If the system is three dimensional, pressure

has its usual meaning. However, for one dimensional systems like the ones we are considering here “tension” is a more appropriate name for our variable, ( $\tau dl$  instead of  $-Pdv$  as mechanical energy or work). With this in mind, we use the word pressure or tension interchangeably.

In Fig.12, we show a state diagram for SG as well as DSG for  $\epsilon = 10$  for the step-like solutions. We note that, as before, the behavior is essentially the same. The pressure increases smoothly from zero and tends to a linear regime with increasing density. This behavior is consistent with the repulsive force diagram (see Fig.7) which shows that the inter-soliton force becomes stronger at short distances which indicates that pressure increases with increasing density.

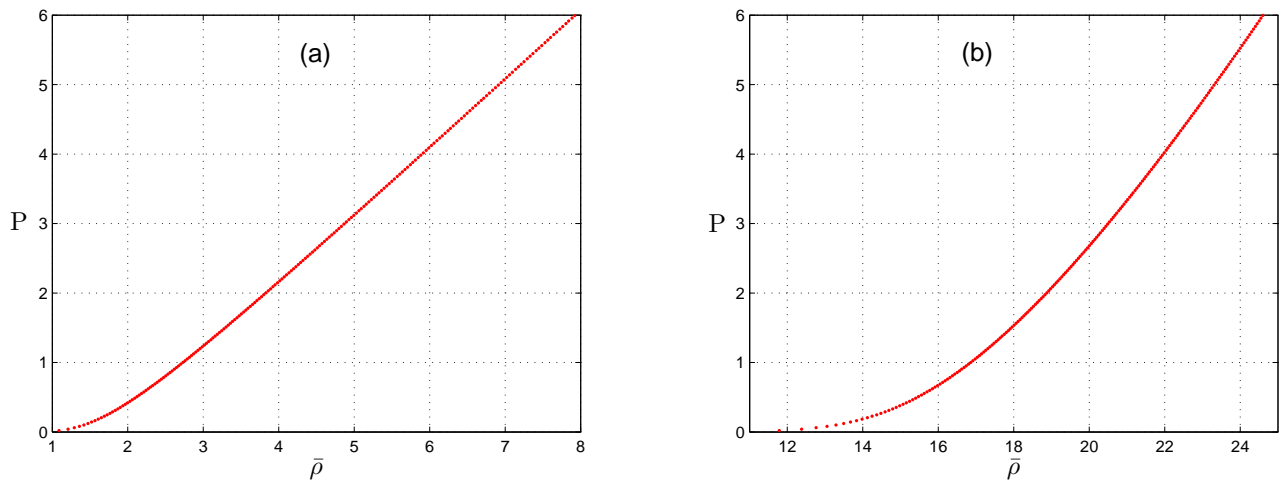


FIG. 12: Equation of state diagram for step-like chain of (a) SG solitons and (b) DSG solitons for  $\epsilon = 10$ .

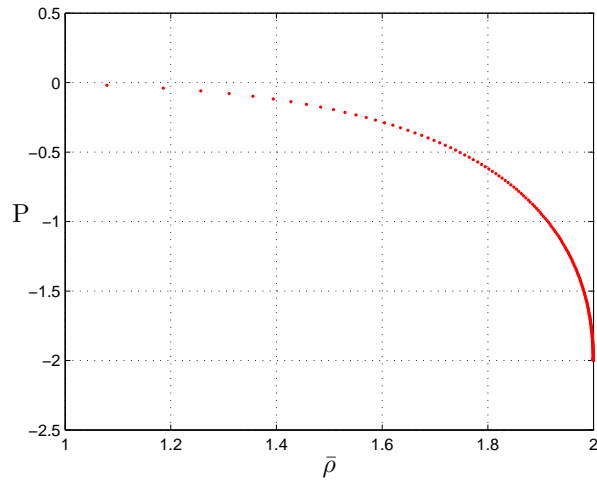


FIG. 13: Equation of state diagram for periodic chain of SG solitons.

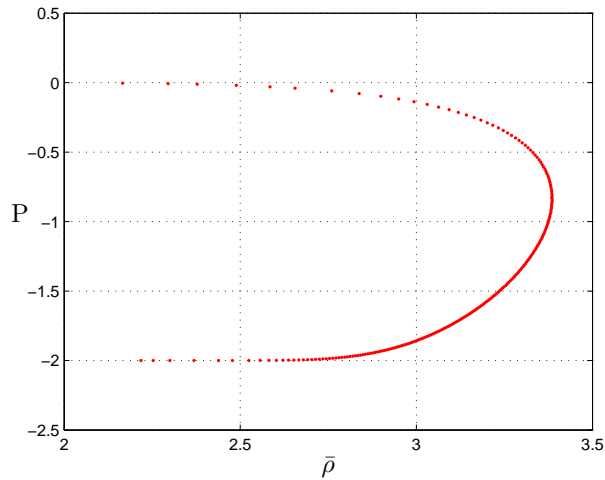


FIG. 14: Equation of state diagram for periodic chain of DSG solitons for  $\epsilon = 1$ . For examples of solutions from each branch see Fig. 10.

As the energy and force diagrams indicate, the state diagrams for periodic chains are more complicated (and therefore more interesting) than the step-like solutions. In Fig.13, we show the state diagram for a periodic chain of SG solitons. Here, with increasing density, the pressure *decreases* from zero. Clearly this negative pressure is a result of attractive force (see Fig.8) among periodic kink-antikink SG solitons. Note that as density increases and inter-soliton distance decreases, the attractive force becomes stronger thus lowering the pressure or increasing the *tension* in this one dimensional chain. The negative value of pressure is simply related to the negative inter-soliton force. An interesting feature of this diagram occurs at  $\bar{\rho} \approx 2$  which is the maximum density. Here,  $P = -2$  and  $\frac{\partial \bar{\rho}}{\partial P} = 0$ , i.e. the “fluid” becomes incompressible. This simply corresponds to an exceedingly large (attractive) force at short distances. We also note that since  $\frac{\partial \bar{\rho}}{\partial P}$  is negative, the term “inexpandable fluid” is perhaps more appropriate than incompressible fluid. Note that the end point  $(P, \rho) = (-2, 2)$  exactly corresponds to the vacuum equation of state  $P = -\rho$ , coming from Eq.(6). Note, however, that this point is highly unstable in the SG system, since it corresponds to a local maximum in Fig.1.

Next, we study the state diagrams for a periodic DSG system. As shown above, the energy diagram splits into two (upper and lower) branches (see Fig.9). Figure 14 shows a typical state diagram for DSG periodic chain. In fact, the state diagram also contains two (connected) branches. The upper half which is similar to the previous state diagram for the simple SG system, as well as a new, lower half which returns the same values of density but at lower pressure values or larger tension. We note that the upper half corresponds to the lower (SG-like) energy branch, whereas

the lower half corresponds to the new upper energy branch of DSG system. Again, it is easy to understand this state diagram in terms of its corresponding force diagram. Here, in the new lower branch, increasing the density (and thus reducing  $L$ ) causes a weaker attractive force (see Fig.11) which in turn causes an increase in the pressure.

The shape of the state diagram, Fig.14, with double-valuedness of pressure is reminiscent of Van der Waals fluid. There, the multiple-valuedness of density as a function of pressure with a corresponding change in the sign of compressibility  $\chi = \frac{\partial \bar{\rho}}{\partial P}$  signals the onset of a liquid-gas transition as temperature is lowered[33]. Our system is obviously very different from that described by the Van der Waals equation of state. However, our system exhibits two distinct solutions, one with a positive and the other with negative  $\chi$ , being joined at a maximum density  $\bar{\rho}_{max} = 3.385$ . This point could be thought of as a phase transition point. The transition point is the point at which the “fluid” becomes “inexpandable”, which separates regimes of different signs of compressibility. In other words, the transition point is the point at which a stable solution ( $\chi > 0$ ) gives way to an (thermodynamically) unstable solution ( $\chi < 0$ ). This can be better seen in Fig.15 where we plot  $\frac{1}{\chi}$  vs.  $P$  in order to show these two distinct phases.

Energy per soliton (Fig.9), and equation of state diagrams (Fig.14) for the periodic chain clearly show two branches. These two branches correspond to two different phases of the chain. The two phases differ in the following respect: The upper branch of Fig.14 corresponds to a chain  $... \tilde{k}k\tilde{k}k\tilde{k}k...$  with solitons separated by a region of true vacuum (zero energy density). This is why at large inter-soliton distances the force (and thus tension) vanishes for this branch. The lower branch, on the other hand, corresponds to pairs of sub-kinks (with vanishing topological charge) separated by regions of false vacuum (non-vanishing energy density). This explains the asymptotic value  $-2$  at low densities (large inter-soliton distances, see fig.11(b)). It is interesting to note that the energy stored in the false vacuum increases linearly with the inter-soliton distance (at large distances) which leads to a constant force (and thus tension). This interesting behavior is reminiscent of the confinement phenomenon in hadronic physics[27].

## V. SUMMARY AND CONCLUSIONS

We have investigated the periodic and step-like solutions of the double-Sine-Gordon equation in this paper. Runge-Kutta algorithm was employed to integrate the static, second order ODE, with adjustable initial conditions ( $\phi = \pi$  and various  $\frac{d\phi}{dx}$  at  $x = 0$ ). The solutions fall into two categories: periodic, and step-like. Step-like solutions are a sequence of kinks ( $...k\tilde{k}k\tilde{k}k...$ ) or anti-kinks ( $... \tilde{k}k\tilde{k}k\tilde{k}k...$ ).

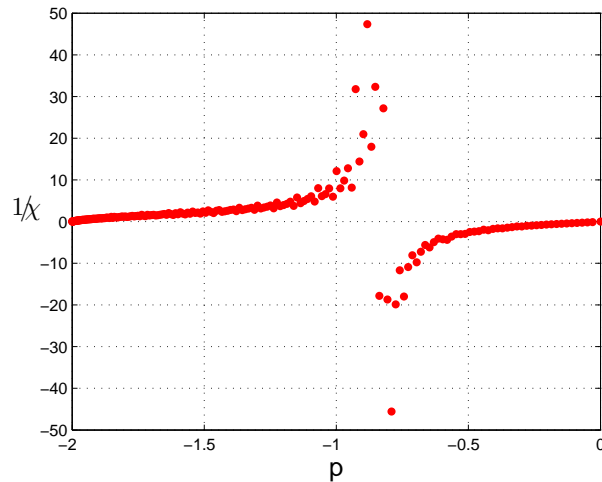


FIG. 15:  $\frac{1}{\chi}$  versus  $P$ , showing clearly two phases with positive and negative values of  $\frac{1}{\chi}$ .

Periodic solutions are a sequence of kink, anti-kink ( $\dots k\tilde{k}k\tilde{k}\dots$ ). For initial conditions considered here, the constant “pressure”  $P$  characterizes these solutions with  $P > 0$  for step-like solutions and  $-2 < P < 0$  for periodic solutions. We also characterize these solutions using their energy density and therefore calculate energy as a function of distance. We are therefore able to consider an “interaction energy” as a function of distance. In this regard, we find that the step-like solutions of DSG equation are similar to their SG counterparts, i.e. the behavior of the system does not change substantially with parameter  $\epsilon$ . However, the behavior of periodic solutions depends crucially on  $\epsilon$ . In fact, we observe the emergence of an extra branch of solutions as  $\epsilon$  is increased.

Using the concept of “interaction energy” we are able to consider our system as an interacting, many-body system on a one dimensional chain at zero temperature. Using standard definitions of pressure and density, we calculate the equation of state for such a system. In this regard, the step-like solutions show standard behavior. However, the periodic solutions show unusual behavior. First, due to the nature of attractive force between them, they exhibit negative pressure. More interestingly, they exhibit a transition from a region of positive compressibility to a region of negative compressibility signifying an intrinsic instability common in many thermodynamic systems exhibiting phase transition. This is of particular interest since most one dimensional interacting systems do not exhibit thermodynamic phase transition.

Many interesting questions arise: Is there an experimental realizations for such a system? We believe that given the prevalence of DSG equation in many experimentally realizable situations outlined in the introduction, there is hope to study such systems experimentally and test our

results.

Furthermore, other generalization are possible. For example, we have looked at potentials of the form  $V(\phi) = 1 + \epsilon - \cos(\phi) - \epsilon \cos(n\phi)$  with  $n$  integer larger than 2, i.e. the multiple Sine-Gordon equation. Here, instead of two branches we obtain multiple branches. Another avenue of investigation is the study of inhomogeneity (e.g.  $\epsilon \neq \text{constant}$ ) in these system. Finally, the role of temperature and fluctuations might be of interest in these systems. Here, the dynamical stability of the solutions we have studied here become an important issue. These issues are currently under investigation and we intend to report our results in forthcoming publications.

### Acknowledgments

N. Riazi and A. Montakhab acknowledge the support of Shiraz University. The authors would like to thank A. Azizi for helpful discussions.

- 
- [1] M. Ishikawa and K. Hide, J. Phys. C: Solid State Phys. (1984).
  - [2] R. Khomeriki and J. Leon, Phys. Rev. **E 71**, 056620 (2005).
  - [3] Gaetano Fiore, math-ph/0512002 (2005).
  - [4] N. Riazi, A. Azizi and S. M. Zebarjad, Phys. Rev **D 66**, 065003 (2002).
  - [5] L. V. Yakushevich, *Nonlinear Physics of DNA*, Wiley,(2004).
  - [6] L. V. Yakushevich, A. V. Savin and L. I. Manevitch, Phys. Rev. **E 66**, 016614 (2002).
  - [7] Sara Cuenda, Angel Sanchez, Niurka R. Quintero, Physica **D 223**, 214221 (2006).
  - [8] J. Timonen, M. Stirland, D. J. Pilling, Yi Cheng, and R. K. Bullough, Phys. Rev. Lett. **56**, 2233 (1986).
  - [9] S. Burdick, M. El-Batanouny and C. R. Willis, Phys. Rev. **B 34**, 6575 (1986).
  - [10] K. Maki and P. Kumer, Phys. Rev. **B 14**, 118 (1976); 14. 3290 (1976).
  - [11] Y. Shiefman and P. Kumer, Phys. Scr. 20, 435 (1979).
  - [12] K. M. Leung, Phys. Rev. **B 27**, 2877 (1983).
  - [13] O. Hudak, J. Phys. Chem. **16**, 2641 (1983); **16**, 2659 (1983).
  - [14] M. El-Batanouny, S. Burdick, K. M. Martini and P. Stancioff, Phys. Rev. Lett. **58**, 2762 (1987).
  - [15] E. Magyari, Phys. Rev. **B 29**, 7082 (1984).
  - [16] J. Pouget and G. A. Maugin, Phys. Rev. **B 30**, 5306 (1984); **31**, 4633(1984).
  - [17] N. Hatakenaka, H. Takayanagi, Y.Kasai and S. Tanda, Physica **B 284-288** (2000) 563-564.
  - [18] T. Uchiyama, Phys. Rev. **D 14**, 3520 (1976).
  - [19] S. Duckworth, R. K. Bullough, P. J. Caudrey and J. D. Gibbon, Phys. Lett. **57 A**, 19 (1976).
  - [20] V. A. Gani and A. E. Kudryavtsev, Phys. Rev. **E 60**, 3305 - 3309 (1999).



- [21] M. Croitoru, J. Phys. A: Math. Gen. **22**, 845-863 (1989).
- [22] Constantine A. Popov, Wave Motion. **42(1)**, 309-350 (2006).
- [23] N. Riazi and A. R. Gharaati, Int. J. Theor. Phys. **37**, 1081 (1998).
- [24] M. Wang and X. Li, Chaos, Solitons and Fractals. **27**, 477 (2006).
- [25] C. A. Condat, R. A. Guyer and M. D. Miller, Phys. Rev. **B 27** , No. 1, 474 (1983).
- [26] L. H. Ryder, *Quantum Field Theory*, Cambridge University Press (1985).
- [27] M. Guidry, *Gauge Field Theories, an Introduction with Applications*, Wiley, NewYork (1991).
- [28] N. Riazi, Int. J. Theor. Phys. GTNO, **8**, No. 2, 115 (2001).
- [29] E. Kreyszig, *Advanced Engineering Mathematics*, John Wiley and Sons, NewYork(1983).
- [30] The lower bound for the value of  $P$ , in general, depends on  $\epsilon$ . However, for the set of initial conditions we consider this lower bound is  $\epsilon$  independent and is equal to  $-2$ .
- [31] Note that from Eq.(6),  $\rho_v = T_0^0 = 2 = \text{constant}$  for the false vacuum and  $E \approx \rho_v \times L$  at large  $L$ .
- [32] R. D'Inverno, *Introducing Einstein's Relativity*, Oxford University Press, NewYork (1992).
- [33] H. B. Callen, *Thermodynamics and an Introduction to Thermostatistics*, John Wiley and Sons, NewYork (1985).